

AD-A222 751

AD _____

SPATIAL RELATIONSHIPS BETWEEN DRUG BINDING SITES ON THE
SURFACE OF THE ACETYLCHOLINE RECEPTOR

David A. Johnson, Ph.D.

Annual Report

October 15, 1986

Support by

U.S. ARMY MEDICAL RESEARCH AND DEVELOPMENT COMMAND

Fort Detrick, Frederick, Maryland 21701-5012

Contract No. DAMD17-84-C-4187

University of California, Riverside

Riverside, California 92521-0121

DTIC
ELECTE
JUN 03 1990

D

Er E

Approved for public release; distribution unlimited

The findings in this report are not to be construed as an official Department of the Army position
unless so designated by other authorized documents.

LIST OF ABBREVIATIONS

ACh	Acetylcholine
AChR	Nicotinic Acetylcholine Receptor
α -toxin	Cobra α -toxin (<i>Naja naja siamensis</i> 3)
FITC	Fluorescein Isothiocyanate
TRITC	Tetramethylrhodamine Isothiocyanate
IEF	Isoelectric Focusing
PCP	Phencyclidine
pI	Isoelectric Focusing Point
NP buffer	100 mM NaCl, 10 mM NaPO ₄ , pH 7.4
HPLC	High pressure liquid chromatography

REPORT DOCUMENTATION PAGE

Form Approved
OMB No. 0704-0188

1a. REPORT SECURITY CLASSIFICATION Unclassified			1b. RESTRICTIVE MARKINGS		
2a. SECURITY CLASSIFICATION AUTHORITY			3. DISTRIBUTION/AVAILABILITY OF REPORT Approved for public release; distribution unlimited		
2b. DECLASSIFICATION/DOWNGRADING SCHEDULE			5. MONITORING ORGANIZATION REPORT NUMBER(S)		
4. PERFORMING ORGANIZATION REPORT NUMBER(S)			7a. NAME OF MONITORING ORGANIZATION		
6a. NAME OF PERFORMING ORGANIZATION University of California-Riverside		6b. OFFICE SYMBOL (if applicable)	7b. ADDRESS (City, State, and ZIP Code)		
6c. ADDRESS (City, State, and ZIP Code) Riverside, California 92521-0121			9. PROCUREMENT INSTRUMENT IDENTIFICATION NUMBER Contract No. DAMD17-84-C-4187		
8a. NAME OF FUNDING/SPONSORING ORGANIZATION U.S. Army Medical Research & Development Command		8b. OFFICE SYMBOL (if applicable)	10. SOURCE OF FUNDING NUMBERS		
8c. ADDRESS (City, State, and ZIP Code) Fort Detrick Frederick, Maryland 21701-5012			PROGRAM ELEMENT NO. 62734A	PROJECT NO. 3M1- 62734A875 ✓	TASK NO. AI
			WORK UNIT ACCESSION NO. 457		
11. TITLE (Include Security Classification) Spatial Relationships Between Drug Binding Sites on the Surface of the Acetylcholine Receptor					
12. PERSONAL AUTHOR(S) David A. Johnson, Ph.D.					
13a. TYPE OF REPORT Annual Report		13b. TIME COVERED FROM 9/15/85 TO 9/14/86		14. DATE OF REPORT (Year, Month, Day) 1986 October 15	
15. PAGE COUNT 50					
16. SUPPLEMENTARY NOTATION					
17. COSATI CODES			18. SUBJECT TERMS (Continue on reverse if necessary and identify by block number)		
FIELD	GROUP	SUB-GROUP	Acetylcholine receptor, cobra a-toxin, fluorescein isothiocyanate, ethidium, anesthetics, fluorescence. RA-V		
19. ABSTRACT (Continue on reverse if necessary and identify by block number) This report is divided into three sections dealing with the development of fluorescent probes of the nicotinic acetylcholine receptor (AChR). Section I summarizes our characterization of the interaction of ethidium with the noncompetitive inhibitory (NCI) site identified by phencyclidine (PCP) binding. Due to an incomplete understanding of the interrelationship between the agonist/antagonist and NCI sites on the AChR, ethidium was originally thought only to interact with the agonist/antagonist sites. However, we show that ethidium, indeed, binds selectively to the NCI site when the AChR is in the desensitized state. Section II deals with our efforts to convert the a-toxin-bound AChR to the desensitized state with butanol. Our hope was that, if the a-toxin bound AChR could be converted to the desensitized state, ethidium could be utilized in conjunction with specifically labelled a-toxins to measure the distances between agonist/antagonist and NCI sites. Section III summarizes our progress to site-specifically label a-toxin with fluorescein isothiocyanate (FITC).					
20. DISTRIBUTION/AVAILABILITY OF ABSTRACT <input type="checkbox"/> UNCLASSIFIED/UNLIMITED <input checked="" type="checkbox"/> SAME AS RPT. <input type="checkbox"/> DTIC USERS			21. ABSTRACT SECURITY CLASSIFICATION Unclassified		
22a. NAME OF RESPONSIBLE INDIVIDUAL Mrs. Virginia M. Miller			22b. TELEPHONE (Include Area Code) 301/663-7325		22c. OFFICE SYMBOL SGRD-RMI-S

SUMMARY

This report is divided into three sections dealing with the development of fluorescent probes of the nicotinic acetylcholine receptor (AChR). Section I summarizes our characterization of the interaction of ethidium with the noncompetitive inhibitory (NCI) site identified by phencyclidine (PCP) binding. Due to an incomplete understanding of the interrelationship between the agonist/antagonist and NCI sites on the AChR, ethidium was originally thought only to interact with the agonist/antagonist sites. However, we show that ethidium, indeed, binds selectively to the NCI site when the AChR is in the desensitized state. Section II deals with our efforts to convert the α -toxin-bound AChR to the desensitized state with butanol. Our hope was that, if the α -toxin bound AChR could be converted to the desensitized state, ethidium could be utilized in conjunction with specifically labelled α -toxins to measure the distances between agonist/antagonist and NCI sites. Section III summarizes our progress to site-specifically label α -toxin with fluorescein isothiocyanate (FITC).

Accession For

NTIS GRA&I ☒

DTIC TAB ☐

Unannounced ☐

Justification

By

Publication

Codes

/or

Special

A-1

1
INSPECTED
QUARTER

FOREWORD

In conducting the research described in this report, the investigators adhered to the "Guide for the Care and Use of Laboratory Animals," prepared by the Committee on Care and Use of Laboratory Animals of the Institute of Laboratory Animal Resources, National Research Council (DHEW Publication No. (NIH) 78-23, Revised 1978).

TABLE OF CONTENTS

	Page No.
DD Form 1473	2
Summary	3
Foreword	4
Table of Contents	5
List of Figures	6
List of Tables	7
Background	8
Section I: Interaction of noncompetitive inhibitors with the acetylcholine receptor: The site and specificity of ethidium binding.	9
Section II: Modulation of receptor state with butanol.	40
Section III: Progress report on efforts to site specifically label cobra α -toxin with FITC.	43
Bibliography	47
List of Abbreviations	50
Distribution List	51

LIST OF FIGURES

Page No.

- 33 Figure 1. Inhibition of the binding of [3 H] PCP by ethidium and its allosteric regulation by agonist occupation.
- 34 Figure 2. The influence of ethidium and PCP on the binding of [3 H] acetylcholine to AChR-enriched membranes.
- 35 Figure 3. Effect of agonist, antagonist and noncompetitive inhibitors on the fluorescence spectra of ethidium bound to the AChR-enriched membranes.
- 36 Figure 4. Fluorescence titration of AChR-enriched membranes with ethidium in the presence of carbamylcholine.
- 37 Figure 5. Dissociation of ethidium-AChR complex in presence of carbamylcholine by PCP.
- 38 Figure 6. The effect of association of carbamylcholine on the binding of ethidium to AChR-enriched membranes.
- 39 Figure 7. Fluorescence lifetime measurements of ethidium bound to AChR-enriched membranes.
- 40 Figure 8. Effect of on butanol on the binding of ethidium to the AChR.
- 45 Figure 9. Photograph of the fluorescence of FITC-toxin monoconjugates resolved on a 0.5 cm thick LKB immoboline gel.
- 46 Figure 10. HPLC elution profile of reduced and S-carboxymethylated peptides from FITC-toxin Band 2 following thermolysin digestion.

LIST OF TABLES

Page No.

- 35 TABLE I. Equilibrium Dissociation Constants for NCI Ligands to Torpedo AChR.
- 31 TABLE II. Fluorescence Spectral Properties of Ethidium Bound to the NCI and Agonist Binding Sites.
- 32 TABLE III. Fluorescence Lifetimes, Amplitudes and Polarization for Ethidium to AChR-Enriched Membranes.

BACKGROUND

Over the last two decades, monumental progress has been achieved in our understanding of the nicotinic acetylcholine receptor. Two major thrusts of research have been toward the elucidation of the receptor structure and of ligand modulation of ion permeability. Current work on the receptor structure includes primary amino acid sequencing of the subunits [9,27,28] and high resolution electron microscopy [19]. The functional responses of interacting ligands are being pursued by now classical binding methods and electrophysiological techniques. We propose to integrate these disparate approaches by utilizing fluorescence energy transfer and quenching techniques as well as peptide mapping and sequencing techniques to examine structural determinants of receptor functional responsiveness. Specifically, we want to measure the topographic disposition of fluorescent agonist/antagonist and noncompetitive blocking agents relative to each and the surface of the lipid bilayer. These goals require a set of fluorescent ligands whose spectroscopic and pharmacological properties are well understood. Since there is an inadequate selection of fluorescent ligands available, our main goal for the last year has been to develop an appropriate set of fluorescent ligands.

In our first annual report, we discussed the characterization of a novel fluorescent probe, decidium, of the agonist/antagonist site on the nicotinic acetylcholine receptor, and summarized our efforts to site-specifically label cobra α -toxin with various fluorophores. In this, the second annual report, we summarize (1) our characterization of the interaction of ethidium with the high affinity noncompetitive inhibitor (NCI) site on the nicotinic acetylcholine receptor, (2) our efforts to convert the α -toxin-bound AChR to the desensitized state, and (3) summarize our efforts to site-specifically label cobra α -toxin with fluorescein isothiocyanate (FITC).

SECTION I

INTERACTION OF NONCOMPETITIVE INHIBITORS WITH THE ACETYLCHOLINE RECEPTOR: THE SITE AND SPECIFICITY OF ETHIDIUM BINDING

A wide variety of ligands has been shown to inhibit the function of the acetylcholine receptor (AChR) in a noncompetitive fashion [40,10]. The tertiary and quaternary amine local anesthetics have been most extensively studied, but the list of noncompetitive inhibitors includes phencyclidine, histrionicotoxin, phenothiazines, gaseous anesthetics, certain basic peptides and several other compounds [7,8,14,45,46]. Detailed electrophysiological studies have shown that these noncompetitive inhibitors reduce the duration of channel open times [25] and enhance the rate of receptor desensitization that follows exposure to agonist [23,41]. Although a single noncompetitive inhibitor can diminish agonist-elicited permeability increases through both mechanisms, the mechanisms differ in the voltage sensitivity and selectivity for ligands of particular structure [20].

The isolation of the acetylcholine receptor in substantial quantities has permitted simultaneous binding and spectroscopic studies of noncompetitive inhibitor association with the receptor. Binding of these ligands is often found to enhance the binding of agonists and occurs at a site or sites distinct from the agonist sites. Thus, these ligands bind at a site allosteric to the agonist-antagonist sites and because the two sites are coupled, they can be regarded as heterotypic inhibitors of receptor function. Although disparate findings have been reported for the stoichiometry of binding these inhibitors, recent studies have shown a single site per receptor monomer to be coupled to agonist binding [15,10].

Little is known about the site of noncompetitive inhibitor binding, although the use of irreversible site-specific labels offers the possibility of defining region(s) responsible for binding of

these ligands within the protein sequence [17,30]. Fluorescence and magnetic resonance spectroscopy also offer the promise of further defining the binding site environment and location of these inhibitors on the intact receptor. However, analysis by fluorescence spectroscopy has been hindered by the lack of selective fluorescent noncompetitive inhibitors [13].

In a search for noncompetitive inhibitors with suitable fluorescence properties, we have re-examined ethidium interactions with the AChR. On the basis of earlier studies, a complex binding mechanism was proposed in which ethidium did not bind either to the noncompetitive inhibitor site or to the agonist sites [34,35]. Should this be case, the information likely to emerge from spectroscopic studies on ethidium would be limited due to the obscure nature of the binding site. However, our analysis of ethidium binding through competitive radioligand binding, fluorescence steady-state titrations, lifetime and polarization analyses show that its mode of interaction with the receptor does not differ from several local anesthetics and typical noncompetitive inhibitors. Thus, ethidium has the requisite specificity for the allosterically-coupled noncompetitive inhibitor site on the AChR and should be a useful probe of receptor function. In this study, we have used the fluorescence properties of ethidium to characterize the molecular nature of the noncompetitive inhibitor binding site.

EXPERIMENTAL PROCEDURES

Materials. [^3H]Phencyclidine (49.9 Ci/mmol) and Na[^{125}I] were purchased from New England Nuclear. [^3H]Acetylcholine (3.7 Ci/mmol) was obtained from Amersham. Ethidium was purchased from Calbiochem-Behring Corp., carbamylcholine and diisopropylfluorophosphate were from Sigma Chemical Co., dibucaine was from ICN Pharmaceuticals, PCP was obtained from the National Institute for Drug Abuse, and H8-HTX was a generous gift of Dr. Y. Kishi (Cambridge, MA). Cobra α -toxin (*siamensis* 3) was isolated by the method of Karlsson et al. [18] from the venom of *Naja naja siamensis*. The lyophilized venom was obtained from Miami Serpentarium. Mono-[^{125}I]iodotyrosine-25- α -toxin was prepared and separated from non-iodinated and diiodo

species by isoelectric focusing [42]. The purity of [^3H]PCP and its co-migration with unlabeled PCP was checked by thin-layer chromatography in n-butanol:acetic acid: H_2O (25:4:10) and subsequent autoradiography on Kodak X-Omat film. All other reagents were of the highest purity available. Live *Torpedo californica* were obtained from Marinus, Westchester, California.

Acetylcholine Receptor Purification. Receptor-enriched membrane fragments were isolated from the electric organ of *Torpedo californica* by established procedures [16] with the following modification: Membranes were base-extracted according to the method of Neubig *et al.* [26] in order to remove peripheral membrane proteins. Specific activities of the receptor preparations were determined by measuring the specific binding of [^{125}I]- α -toxin receptor to DEAE-cellulose filters [36]. Specific activities for the receptor ranged from 1.0-2.2 nmol of α -toxin binding sites/mg protein.

Binding of [^3H]PCP. The equilibrium binding of radiolabeled PCP was measured as described by Heidmann *et al.* [15] with the following modifications. AChR-enriched membranes were suspended in 100 mM NaCl, 10 mM NaPO_4 , pH 7.4 at a final concentration of 1.0 μM α -toxin sites. Binding of [^3H]PCP was determined under the following conditions: 1) membranes were not treated with cholinergic ligand prior to [^3H]PCP addition, 2) a 10-fold molar excess of α -toxin was incubated with AChR for 1 hr prior to addition of [^3H]PCP, and 3) 200 μM carbamylcholine was incubated with AChR for at least 10 min prior to the addition of [^3H]PCP. Nonspecific binding was determined from bound [^3H]PCP in the presence of 1 mM PCP. A 20 μM [^3H]PCP stock solution was prepared so that the ratio of the concentrations of radiolabeled to unlabeled PCP was 0.05. The final concentration of [^3H]PCP in the samples was 1.0 μM . After addition of the noncompetitive inhibitor, samples were incubated for at least 1 hr at 20°C in Beckman polyallomer airfuge tubes. Bound ligand was separated from free ligand by ultracentrifugation in a Beckman airfuge for 5 min at 30 psi (160,000 x g). Duplicate 10 μl aliquots of the supernatant were removed, or alternatively, aliquots were withdrawn prior to centrifugation to determine total counts. The

supernatant was then aspirated, and a 3 mm end of the tube containing the pellet was cut off. The membrane pellets and supernatant aliquots were solubilized and counted in 5 ml of Bioflor (NEN) using a LKB 1211 Rackbeta.

Binding of [3 H]ACh. Binding of [3 H]ACh to Torpedo membranes was measured using the ultracentrifugation sequence and buffer described above. To prevent [3 H]ACh hydrolysis, acetylcholinesterase was inactivated by treatment of a concentrated membrane suspension (2.5 μ M α -toxin sites) with 1 mM diisopropylfluorophosphate (DFP) for 1 hr at 25°C. Binding studies were subsequently conducted in the presence of 10 μ M DFP. AChR membranes (25 nM α -toxin sites) and [3 H]ACh were incubated in the presence or absence of noncompetitive inhibitors for 1 hr at 25°C. Non-specific binding of [3 H]ACh was determined by incubating the AChR with 10-fold excess α -toxin for 1 hr. After ultracentrifugation, free [3 H]ACh was removed by aspiration. The membrane pellet containing bound [3 H]ACh was then solubilized by addition of 30 μ l 10% (w/v) Triton X-100 for at least 18 hr and counted as described above.

Fluorescence Titrations. Steady state fluorescence measurements were made on a Spex Fluorolog 2 interfaced to a Spex DM1B computer. The light source was a 150W xenon-arc lamp and fluorescence was detected by photon counting. Fluorescence spectral intensities were the ratio of excitation to reference intensities and thus corrected for lamp spectral shape. Emission spectra were corrected for wavelength-dependent throughput detector sensitivity. Typical excitation and emission slits yielded a bandpass of 4.6 nm. Titrations were performed in 100 mM NaCl, 10 mM NaPO₄, pH 7.4 in 1 cm² cuvettes. Aliquots of ethidium or other ligand were added from a Hamilton syringe. One of four cuvettes that routinely contained ethidium in buffer was used to correct for dilution from added titrant. Typically, ethidium fluorescence was measured by employing excitation wavelengths of either 290 nm or 500 nm while monitoring emission at 594 nm. Excitation at 290 nm required the use of a Corning 7-54 filter on the excitation side and a Corning 3-70 cutoff filter on the emission side.

Analysis of Ligand Binding. Radioligand competition binding experiments were analyzed by a weighted non-linear regression computer program, LIGAND for a single class of binding sites [24]. We used values of 0.4 μM for the K_D of PCP in the presence of carbamylcholine and 2.0 μM in the presence of α -toxin. Data points are the average of duplicate samples. Figures show the results of individual experiments each of which was performed at least three times with different membrane preparations. Dissociation constants for nonfluorescent competing ligands were derived from analysis of their capacity to displace the fluorescent ligand, ethidium. Fluorescence data were plotted according to a logarithmic formulation [39]:

$$\log\left[\frac{f_E - f}{f - f_C}\right] = n_H \log\frac{K_E}{K_C} + n_H \log\frac{[C]}{[E]} \quad (\text{Equation 1})$$

where f_E denotes the initial fluorescence in the absence of competing ligands, f_C denotes the fluorescence when ethidium is completely displaced from the AChR, and f denotes the fluorescence observed at any given concentration of competing ligand. $[E]$ and $[C]$ represent free concentrations of ethidium and competing ligand, and K_E and K_C their respective dissociation constants. Dissociation constants for the nonfluorescent competing ligands (K_C) were calculated from the intercept on the abscissa and K_E . The logarithmic relationship of equation 1 is formally analogous to the Hill equation, and a slope (n_H) that differs from unity should reflect either heterogeneity in binding sites or cooperativity in binding.

Steady-State Polarization. Fluorescence polarization was measured with [3M] polarizers in the excitation (520 nm) and emission (600 nm) light paths. Fluorescence polarization, P , was calculated according to the following equation:

$$P = \frac{I_{VV} - G \cdot I_{VH}}{I_{VV} + G \cdot I_{VH}} \quad (\text{Equation 2})$$

where I is the fluorescence intensity, the first and second subscripts refer to the vertical (V) or horizontal (H) orientation of the excitation and emission beams, respectively. The factor G

(I_{HV}/I_{HH}) corrects for the unequal transmission of the vertical and horizontally polarized light by the instrument diffraction gratings. Samples containing AChR-enriched membranes were corrected for light scatter by subtracting intensities measured in cuvettes which contained AChR-enriched membranes in the absence of ethidium.

Fluorescence Lifetime Analysis. Fluorescence lifetimes were determined by the single-photon counting technique using an EBY scientific nanosecond fluorometer (La Jolla, CA) equipped with a high-pressure hydrogen arc lamp. Data were accumulated in an E.G.G. Ortec 7150 multichannel analyzer (Salem, MA), analyzed, and displayed by using an IBM-PC computer and a Hewlett Packard 7470A plotter (San Diego, CA). For excitation in the UV region, excitation and emission bands were selected with Corning 7-54 and 3-70 cut-off filters (Corning, NY), respectively. For excitation in the visible band, an Oriel broad-band 450 nm (No. 5754) interference and a Corning 2-73 cut-off filter were used. In addition to the chromatic filters, Polaroid HNP'B dichroic film polarizers (Norwood, MA) were placed in the excitation and observation paths. The emission polarizer was rotated at an angle of 55° relative to the vertically oriented excitation polarizer to eliminate anisotropic contributions to the observed decay. The instrumental arrangement and principles of data treatment have been discussed in detail [44].

The intensity $[I(t)]$ versus time relationship, directly measured with the nanosecond fluorometer, is distorted by the finite duration of the lamp pulse $[L(t)]$, and is related to the undistorted time course of emission $[F(t)]$ by the convolution integral (Eq. 3).

$$I(t) = \int_0^t L(T)F(t-T)dT \quad (\text{Equation 3})$$

The lamp profile $L(T)$ was measured with a light scattering solution in the sample compartment in place of the fluorophore sample with the emission filter removed. $F(t)$ was obtained from measured values of $I(t)$ and $L(t)$ by deconvolution with the method of moments, assuming that $F(t)$ can be represented by a one- or two- exponential expression. For a two-exponential fluorescence

decay function, the fluorescence lifetimes (τ_1 and τ_2) and their pre-exponential factors (a_1 and a_2) are given by:

$$F(t) = a_1 \exp(-\frac{t}{\tau_1}) + a_2 \exp(-\frac{t}{\tau_2}) \quad (\text{Equation 4})$$

The time shift between $L(t)$ and $I(t)$ introduced by the spectral response properties of the detecting photomultiplier tube was corrected with a time-shift introduced by the computer. Convolution of $F(t)$ so obtained with $L(t)$ generates a new function $C(t)$ which can be compared with $I(t)$. Values of coefficients and lifetimes are chosen so that the reduced χ^2/N is a minimum.

$$\frac{\chi^2}{N} = \frac{1}{N-n} \sum \frac{1}{\sigma_i^2} [I(t_i) - C(t_i)]^2 \quad (\text{Equation 5})$$

where χ_i is the standard deviation of $I(t_i)$ due to noise, N is the total number of data points, and n is the number of fitted parameters.

RESULTS

Ethidium Inhibits the Binding of [3H]PCP and Is Allosterically Regulated by Occupation of the Agonist Site. To determine directly whether ethidium binds to a noncompetitive inhibitor site on the AChR, the capacity of ethidium to inhibit [3H]PCP binding was measured. [3H]PCP was selected as a marker of the high-affinity noncompetitive inhibitor site since its stoichiometry of binding has been precisely determined and its interactions with other sites show markedly lower affinities [15]. In agreement with others [15], we found that at concentrations less than 20 μM , [3H]PCP binds to a single class of binding sites on AChR-enriched membranes either in the presence of carbamylcholine ($K_D = 0.4 \mu\text{M}$) or in the presence of α -toxin ($K_D = 2.0 \mu\text{M}$). We also confirmed that the stoichiometry of [3H]PCP binding is approximately one per receptor monomer (0.82 ± 0.17) [15].

Because previous studies have shown that the binding of many noncompetitive inhibitors is

allosterically regulated by occupation of the agonist site, we examined competition of ethidium with $[^3\text{H}]\text{PCP}$ in the presence of carbamylcholine and α -toxin (Fig. 1). The large excess of carbamylcholine or stoichiometric excess of α -toxin precludes the possibility of ethidium binding to the agonist site and hence affecting the observed dissociation constants. As shown in Fig. 1, in the presence of carbamylcholine, ethidium competes with $[^3\text{H}]\text{PCP}$ with high affinity ($K_D = 0.36 \mu\text{M}$) and the data fit a single class of binding sites (solid line). Ethidium in the presence of α -toxin exhibited substantially lower affinity for competing with PCP, with a $K_D = 1,000 \mu\text{M}$. Thus, these data show a pattern of allosteric regulation by the agonist site for ethidium binding typical of many noncompetitive inhibitors, including quaternary amine local anesthetics [15,21].

Allosteric Behavior and Binding of Ethidium to the Agcnist Sites. To determine directly the heterotropic effects of ethidium on the agonist sites, a subsaturating concentration of $[^3\text{H}]\text{ACh}$ was used to occupy a fraction of the agonist sites. Under these conditions, conversion of the agonist sites from low affinity ($K_D = \sim 1 \mu\text{M}$) in the resting state to high affinity ($\sim 8 \text{ nM}$) characteristic of the desensitized state, yields a 400% increase in the amount of $[^3\text{H}]\text{ACh}$ bound. As seen in Fig. 2a, increasing concentrations of PCP produce a monophasic increase in the amount of $[^3\text{H}]\text{ACh}$ bound at equilibrium. In contrast, increasing concentrations of ethidium generate a bell-shaped curve; low concentrations ($< 10 \mu\text{M}$) increase agonist binding while higher concentrations inhibit binding. Similar biphasic curves have been observed with several aromatic amine local anesthetics [21]. This bell-shaped curve may be explained as a combination of two distinct processes: 1) at low concentrations, ethidium binds at the noncompetitive site and its occupation converts the receptor to a state with high affinity for agonists, and 2) at high concentrations, ethidium competes directly at the agonist sites. Consistent with this interpretation, the values of the dissociation constants for PCP and ethidium increasing $[^3\text{H}]\text{ACh}$ binding closely correspond to the K_D s for these compounds binding to the noncompetitive inhibitor site (Table I).

To resolve the two putative binding components of the bell-shaped ethidium curve, we directly

measured the competition at the agonist sites. In this case, saturating concentrations of [^3H]ACh were employed to convert the receptor to the high-affinity, desensitized state; thus, ethidium binding at the noncompetitive inhibitor site should not further enhance binding. Figure 2B shows the concentration dependence of the inhibition of [^3H]ACh binding. The competition binding between a saturating concentration of [^3H]ACh and ethidium was also examined in the presence of a large excess of PCP (250 μM) in order to block ethidium interaction at the noncompetitive inhibitor site. Similar competition binding isotherms were obtained in the two experiments and dissociation constants of ethidium for the agonist site of $18 \pm 0.4 \mu\text{M}$ in the absence of PCP and $11 \pm 2.5 \mu\text{M}$ in the presence of PCP were calculated for a single class of binding sites. These results show that the relative affinity of ethidium for the agonist site is 40- to 70-fold lower than the affinity for the noncompetitive inhibitor site in the desensitized state.

Fluorescence Spectra of Ethidium Bound to the Noncompetitive Inhibitor Site.

Fluorescence spectra of ethidium were substantially altered upon binding to the noncompetitive inhibitor site and were dependent on the functional state of the receptor. Excitation spectra of ethidium obtained in the presence of 1 mM carbamylcholine showed a large increase in fluorescence intensity upon binding to the receptor relative to ethidium in buffer (Fig. 3A). At the same time, the excitation maximum shifted from 480 nm, characteristic of ethidium in buffer, to ~ 527 nm. Addition of a large excess of PCP (1 mM) to receptor previously equilibrated with ethidium and carbamylcholine resulted in a large reduction in fluorescence intensity. A similar decrease in intensity was seen with addition of a stoichiometric excess of α -toxin. The excitation spectra in the presence of either α -toxin or PCP showed an excitation maximum at 503 nm, a value intermediate between the maxima observed in the presence of carbamylcholine or buffer alone.

The emission spectra of ethidium bound to AChR membranes showed parallel changes in fluorescence intensity and concomitant shifts in wavelength maxima. Excitation of ethidium in buffer in the visible band at 480 nm produced a low intensity emission centered at 635 nm (Fig. 3B).

Binding of ethidium to the AChR-enriched membranes in the presence of carbamylcholine resulted in a large enhancement in emission and a blue-shift in the spectrum to 598 nm. Addition of either 1 mM PCP or a 10-fold molar excess of α -toxin resulted in a large decrease in the fluorescence emission and red-shift in the emission maxima to 620 nm. For comparison, emission spectra were also obtained by exciting at 290 nm, where energy transfer from protein tryptophan residues to ethidium should occur in addition to direct excitation (Fig. 3C). As in the case of excitation in the visible band, the emission intensity in the presence of carbamylcholine was greatly enhanced in intensity and exhibited a 35 nm blue shift in the maximum, while in the presence of either PCP or α -toxin, emission was of lower intensity and shifted to the blue by only 15 nm. The greater enhancement in fluorescence emission observed for 290 nm versus 480 nm excitation reflects energy transfer from protein tryptophan residues to ethidium bound at the noncompetitive inhibitor site. Excitation spectra of ethidium show a strong absorption band between 300-355 nm which overlaps tryptophan fluorescence emission. Energy transfer was confirmed by measuring a specific decrease (12%) in the tryptophan fluorescence emission ($\lambda_{\text{max}} = 338$ nm) from AChR-enriched membranes in the presence of ethidium (data not shown).

We have defined nonspecific binding in this study with respect to two independent criteria: 1) displacement by saturating concentrations of noncompetitive inhibitor ligand, and 2) by converting the noncompetitive inhibitor site to a state of very low affinity for ethidium with α -toxin. The nonspecific binding that remains under these conditions would be primarily composed of the nonsaturable partitioning of ethidium into the bulk lipid phase of the AChR-enriched membranes. Part of the nonspecific binding may also include the association of ethidium with the lipid-AChR interfacial region. Since the ethidium emission spectra obtained in the presence of carbamylcholine are composite spectra composed of specific and nonspecific components, spectral subtraction was carried out to visualize the specific component. As seen in Fig. 3D, difference spectra were generated by subtracting the nonspecific component defined either by excess PCP or by saturating

levels of α -toxin. In both cases, the spectral shape and emission maxima of the difference spectra were identical ($\lambda_{\text{max}} = 598 \text{ nm}$). The difference emission spectra obtained by excitation at 290 nm or at 480 nm also had similar spectral line shape and emission maxima. Thus, the noncompetitive inhibitor site as identified by spectral criteria is the same when specific binding is defined either with reference to excess noncompetitive inhibitor or by converting the receptor to a low-affinity state by dissociating agonist with α -toxin.

Spectral properties of ethidium bound only to the agonist sites were determined in the presence of saturating concentrations of PCP. Excitation spectra showed a maximum at 504 nm. This value is significantly different from ethidium bound at the noncompetitive inhibitor site, but does not differ appreciably from the maxima for nonspecifically bound ethidium. Emission spectra ($\lambda_{\text{ex}} = 290 \text{ nm}$) of ethidium bound at the agonist site exhibited a much smaller increase in fluorescence intensity compared to the noncompetitive inhibitor site. Excitation in the UV and visible both produced similar emission maxima that did not differ greatly from maxima obtained for nonspecific binding in the presence of either excess agonist or α -toxin, but difference spectra showed a maxima at 614 nm. Thus, the fluorescence intensities, as well as excitation and emission maxima are significantly different for ethidium bound to the noncompetitive inhibitor and agonist binding sites.

Fluorescence Titrations of Ethidium Association with AChR-Enriched Membranes. To characterize the interactions of ethidium with the noncompetitive inhibitor site, fluorescence titrations were performed using AChR-membranes in the presence of 0.5 mM carbamylcholine. As seen in Fig. 4A, the total binding of ethidium could be resolved into a hyperbolic saturable binding isotherm superimposed on a linear, nonspecific component. The nonspecific fluorescence component was identified by titrations either in the presence of excess PCP or a 10-fold excess of α -toxin, and found to be identical. Subtraction of the linear component defined by either excess competing ligand or by maintaining the binding site in a low-affinity conformation yielded equivalent

saturable binding components. A Scatchard plot of these data shown in Fig. 4B indicates that ethidium binds to a single class of non-interacting sites distinct from the agonist binding sites with a dissociation constant equal to $0.25 \mu\text{M}$. The dissociation constant determined by fluorescence was in reasonable agreement with the corresponding value of $0.36 \mu\text{M}$ determined by competition with $[^3\text{H}]\text{PCP}$.

The stoichiometry of the high-affinity ethidium binding sites was determined by fluorescence titration under conditions where the number of ethidium binding sites was in large excess over the K_D for ethidium (Fig. 4C). In this experiment, substantial light scattering due to the membrane fragments limited the concentration of sites that could be used for titration. Extrapolation of the linear increase in specific fluorescence intensity which reflects ethidium binding stoichiometrically, to the level reached at saturation yielded an estimate of $0.90 \pm 0.1 \mu\text{M}$ for the ethidium site concentration. Since the concentration of α -toxin sites was $2.0 \mu\text{M}$, the number of ethidium sites is equal to half the number of α -toxin sites.

Dissociation of Bound Ethidium by Noncompetitive Inhibitor Ligands. Figure 5A and B show back titrations of ethidium fluorescence by well-characterized noncompetitive inhibitors when the agonist sites are saturated with carbamylcholine. As seen in Fig. 5A, competitive dissociation of ethidium by PCP was directly monitored by a decrease in ethidium fluorescence at 593 nm upon excitation at 500 nm and yielded an apparent IC_{50} of $1.5 \mu\text{M}$. The fluorescence intensity reached at saturating concentrations of PCP was equal to that obtained in the presence of excess α -toxin. Similar dissociation curves were obtained using H8-HTX and dibucaine in back-titrations, and the fluorescence intensities obtained at saturating concentrations of all three competing ligands were the same. The fluorescence back titration data for PCP, H8-HTX and dibucaine were analyzed by Equation 1 (Fig. 5B). Table I shows that the dissociation constants calculated for the competing ligands were found to closely agree with values determined by direct radioligand binding (for $[^3\text{H}]\text{PCP}$) and by competition binding with $[^3\text{H}]\text{PCP}$ (H8-HTX and dibucaine). Cohen and

coworkers (1985) have also found that ethidium displaced [^3H]HTX in the presence carbamylcholine with a 1C_{50} of $\sim 1\ \mu\text{M}$. The competitive titration curves exhibit slopes in the logarithmic plots that are not significantly different from unity (Table I). Since equation 1 is based on a competitive relationship between ethidium and the associating ligand, slopes of unity indicate that the competing ligands bind to a homogeneous class of independent sites in causing ethidium dissociation.

Effect of Ligand Occupation of the Agonist/Antagonist Site on Ethidium Fluorescence.

An additional characteristic of the ethidium fluorescence signal from the noncompetitive inhibitor site should be the allosteric regulation by agonists, as previously demonstrated by competition binding with [^3H]PCP (Fig. 1). To determine the effect of agonists on ethidium fluorescence originating from the noncompetitive inhibitor site, titrations with carbamylcholine were performed (Fig. 6). The specific fluorescence change was calculated by correcting for nonspecific changes that occurred in the presence of a fivefold excess of α -toxin. In this experiment, the concentration of agonist sites was approximately equal to the K_D of carbamylcholine. The solid line through the data is a theoretical curve calculated from the law of mass action for a carbamylcholine dissociation constant of $1.4\ \mu\text{M}$ assuming an equivalence of carbamylcholine and α -toxin sites. The apparent dissociation constant obtained from this curve is similar to the K_D obtained from the inhibition of the initial rate of α -toxin binding by carbamylcholine after equilibrium exposure (Weiland, 1979). A Hill plot of carbamylcholine titration data indicated a Hill coefficient significantly greater than unity ($n = 1.27 \pm 0.10$). This suggests that modest positive cooperativity between subunits involved in the association of carbamylcholine is monitored by ethidium at the noncompetitive inhibitor site.

Fluorescence Lifetime Analysis. The fluorescence lifetime of ethidium bound to the noncompetitive inhibitor site was examined in order to clarify the mechanism responsible for the increase in fluorescence intensity that occurs upon carbamylcholine binding. UV excitation was employed to enhance the contribution of the specifically bound ethidium fluorescence. As seen in Fig. 7C, the fluorescence decay rate for ethidium in buffer followed a single exponential function.

The lifetime was calculated to be 1.7 ns, in good agreement with previously determined values (Olmsstead and Kearns, 1977). The corresponding fluorescence decay rates of AChR-membranes containing ethidium bound at the noncompetitive inhibitor site (Fig. 7A) and nonspecifically bound (Fig. 7B) showed dramatic increases in fluorescence lifetimes (Table II). For ethidium bound to the AChR at the noncompetitive inhibitor site, only a single exponential was required to fit the decay, yielding a lifetime of 22.2 ns. However, the fluorescence decay curve of ethidium under conditions of nonspecific binding did not follow a single exponential decay behavior, but was described by an equation containing two exponential terms (Equation 5). The fluorescence decay was characterized by a short lifetime component ($\tau_1 = 1.8$ ns) and a longer lifetime component ($\tau_2 = 22.1$ ns) with a ratio of amplitudes (a_1/a_2) of 7.5. The short lifetime was nearly identical to that observed for ethidium only in buffer, which indicated that PCP displaced ethidium from its binding site into the aqueous phase. The preexponential factors (a_1 and a_2) give the fractional population of each component, which in this case correspond to free (a_1) and nonspecifically bound (a_2) ethidium. AChR and ethidium in the presence of excess α -toxin also showed two-exponential decay behavior with nearly identical lifetimes and ratio of preexponential factors. Titration of AChR with ethidium to achieve fractional occupation of the noncompetitive inhibitor site showed a rough correspondence between the decrease in the a_1/a_2 ratio and site occupation (data not shown).

The assignment of free, specifically bound, and nonspecifically bound lifetime components is supported by lifetime analysis of data obtained from the above samples by excitation in the visible band. In contrast to the data obtained by UV excitation, the fluorescence decay for ethidium bound at the noncompetitive inhibitor site clearly required a two-exponential fit. A short lifetime component ($\tau_1 = 2.3$ ns) corresponding to ethidium in buffer was observed in addition to the longer lifetime component ($\tau_2 = 21.9$ ns) characteristic of specifically bound ethidium ($a_1/a_2 = 2.5$). This long lifetime component corresponded to the same lifetime observed with UV excitation. Addition of 1 mM PCP greatly increased the ratio of the free-to-bound amplitudes ($a_1/a_2 = 18.5$) while not

changing the two lifetime values. Thus, the single exponential decay found for specifically bound ethidium with UV excitation can be attributed to the selective excitation of ethidium bound to the noncompetitive inhibitor site that is due to energy transfer from protein tryptophan residues.

Steady-State Polarization of Ethidium Fluorescence. The mobility of ethidium bound to the noncompetitive inhibitor site was determined by steady-state fluorescence polarization measurements. Ethidium was excited in the main visible transitions located at 480 nm in buffer and at 520 nm when bound to the noncompetitive binding site. As seen in Table III, ethidium polarization in buffer is negligible as expected for a small fluorophore undergoing rapid isotropic rotation. Ethidium (1.0 μM) bound to AChR (1.0 μM α -toxin sites) in the presence of saturating concentrations of carbamylcholine shows an extremely high polarization value, $P = 0.4 \pm .01$. In the case of ethidium binding to the AChR in the presence carbamylcholine, the large enhancement in fluorescence upon binding weights the steady-state polarization measurement in favor of the specifically bound ligand population. A Perrin plot of ethidium in buffer was used to determine a limiting polarization (P_0) value of 0.40 (data not shown). Ethidium bound to the noncompetitive inhibitor site approaches the maximal limiting polarization value, indicating its strong immobilization. Addition of a large excess of PCP to the specifically bound ethidium AChR-carbamylcholine complex resulted in a substantial decrease in polarization to 0.22 ± 0.01 . Moreover, prior incubation of AChR with excess α -toxin also significantly decreased the ethidium polarization to 0.27 ± 0.01 . The similar reductions in polarization for ethidium in the absence of specific binding partly reflect the displacement of ethidium from its binding site and transfer to the aqueous phase. The intermediate polarization value also indicates that the remaining nonspecifically bound ethidium is also substantially immobilized.

DISCUSSION

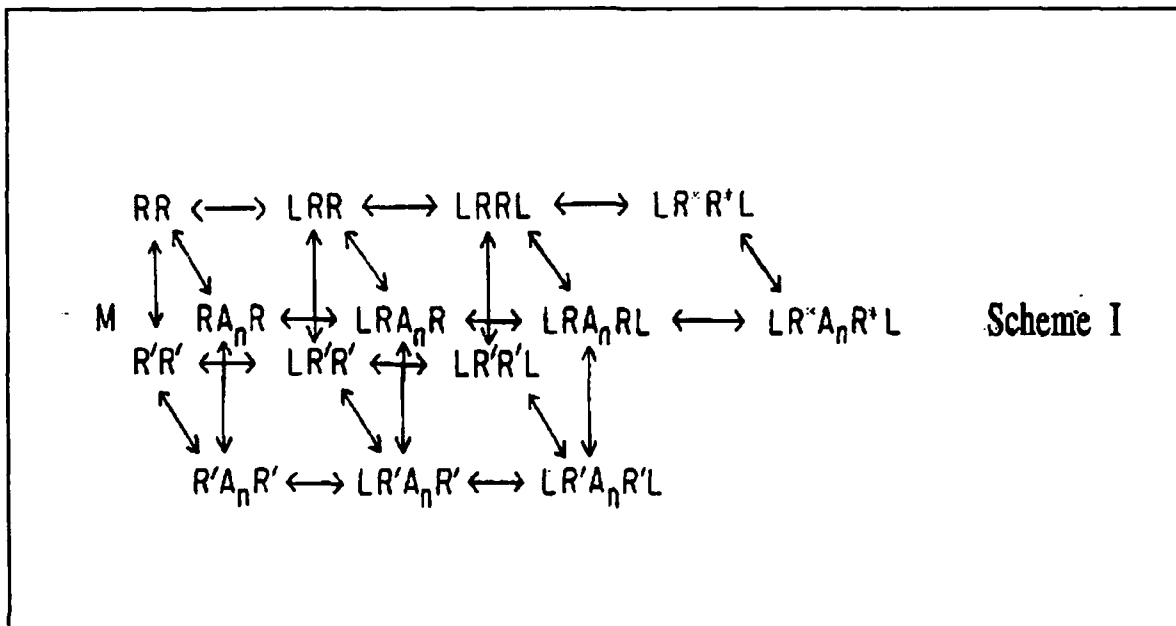
Our study demonstrates that ethidium can be utilized as a specific fluorescence probe of the noncompetitive inhibitor site on the AChR from *Torpedo californica*. Both radioligand competition

binding and direct fluorescence titrations show that ethidium binds to a single site, distinct from the agonist binding sites, whose affinity is allosterically regulated by agonist binding. Binding of ethidium to the noncompetitive inhibitor site also converts the receptor to a state exhibiting increased agonist affinity. The noncompetitive inhibitor ligands, PCP, H8-HTX, and dibucaine, were found to completely displace specifically bound ethidium, indicating a common binding site for all four ligands.

An important issue in the study of noncompetitive inhibitor binding to the AChR concerns the number and classes of binding sites, and their coupling to transitions in receptor states. Radiolabeled derivatives of phencyclidine and HTX bind with high affinity to a single class of sites which are allosterically coupled to the agonist binding sites. The stoichiometry of this allosterically coupled site has been found to be one per receptor monomer [10,15]. In addition to binding to the single allosterically regulated site, some noncompetitive inhibitors such as [^{14}C]meproadifen, [^3H]trimethisoquin, and [^3H]chlorpromazine also bind to a second class of sites that have lower affinity and greater numbers, and do not show coupling to the agonist sites [15,21,38]. We find that ethidium binds only to the first class of allosterically-regulated sites with a stoichiometry of one per receptor. Since no binding to a second class of noncompetitive inhibitor sites could be detected, ethidium represents an ideal fluorescent probe for characterizing specific binding sites identified by PCP and HTX binding.

A quantitative description for a two-state cyclic scheme for receptor desensitization has been deduced from extensive studies of the influence of local anesthetics and agonists on the kinetics of AChR state transitions [42,43,14,5,37]. Our results can be considered with respect to an expanded coupled-equilibria model which describes the molecular species and influence of agonists and noncompetitive inhibitors on receptor states. In this model, the AChR contains two agonist (L) binding sites (RR) and a topographically distinct binding site(s) for the allosteric, noncompetitive inhibitor (A). As indicated in Scheme I, within the time frame in which we are working the AChR

can be thought to exist in at least three distinct states, which are: resting (RR), activated or open channel (R^*R^*) and desensitized ($R'R'$).



The sequential binding of two agonists (L) to the receptor in the resting state will lead to the rapid activation of receptor cation permeability via the LR^*R^*L species. In the continued presence of agonist, the receptor is converted to the desensitized state ($LR'R'L$) in which the channel is refractory to opening. While the noncompetitive inhibitors such as local anesthetics may interact with all three receptor states, studies have shown that these allosteric ligands primarily inhibit AChR function by influencing conductance and duration of the open channel state (LR^*AR^*L) or by stabilizing the desensitized receptor state (R'). The desensitized receptor state is characterized by having a higher affinity for agonists and most local anesthetics. Sine and Taylor (1982) have shown that HTX and several local anesthetics increase the allosteric constant (M) at concentrations that induce desensitization and block the AChR permeability response. In the presence of a noncompetitive inhibitor the allosteric constant (M') is given by:

where M, the allosteric constant, equals $R'R'/RR$, and defines the ratio of receptor in the

$$M' = M \left[\frac{1 + \frac{[A]}{K_{R'A}}}{1 + \frac{[A]}{K_{RA}}} \right] \quad (\text{Equation 6})$$

desensitized to resting state in the absence of agonist and allosteric ligand. $K_{R'A}$ and K_{RA} are the dissociation constants for the heterotypic ligand, A, binding to the allosteric site of the AChR in the R'R and RR states. Allosteric inhibitors that show the highest selectivity for binding to R'R' will show the largest increase in M' . Thus, through these coupled equilibria, agonists can act to increase the affinity of anesthetics, and conversely, anesthetics can increase the affinity of agonists for the receptor.

An additional characteristic of ethidium binding, typical of PCP, HTX and many aromatic amine local anesthetics, is a preference for binding to the desensitized receptor state. However, ethidium is distinctive in showing the largest selectivity ratio of many compounds examined in Torpedo, since $K_{RA}/K_{R'A} > 2700$. By comparison, the $K_{RA}/K_{R'A}$ ratios for H8-HTD and PCP do not exceed 5 [15]. Similarly, many aromatic amine local anesthetics are bound about one order of magnitude more tightly to the desensitized receptor state [3,15,1].2 As previously noted for a homologous series of compounds [4], it appears that small differences in structure between noncompetitive inhibitors may dramatically affect binding preferences for the resting and desensitized receptor states.

In previous studies on ethidium binding to the AChR., Raftery and coworkers proposed that ethidium binding did not occur at either the agonist or the noncompetitive inhibitor sites [34,35,11,33]. They found that several local anesthetics decreased ethidium fluorescence in the absence of agonist. A complex mechanism was proposed for local anesthetic interaction with the AChR that was based upon an induced conformational change in an ethidium-AChR complex that decreased quantum yield of bound ethidium. It was also concluded that the fluorescence increase associated with carbamylcholine addition is due to an increase in the quantum yield of a pre-existing

ethidium-AChR complex [34]. However, since many of these experiments were carried out in the absence of agonist, ethidium could have exhibited significant binding to the agonist sites. Since local anesthetics, which include lidocaine, tetracaine and dibucaine, have been shown to bind to the agonist sites at higher concentrations [3], changes in fluorescent signal may have resulted from competition between local anesthetics and ethidium at the agonist sites.

Our fluorescence lifetime measurements and binding data provide strong evidence that the mechanism for fluorescence enhancement by carbamylcholine is an increase in specifically-bound ethidium at the noncompetitive inhibitor site. Greater fractional occupation by ethidium is due to a large enhancement in affinity at that site. First, as a result of binding to the non-competitive inhibitor site, the quantum yield for ethidium increases over 14-fold compared to ethidium free in solution. Secondly, the fluorescence back titration data show that ethidium bound at this site is dissociated completely by several noncompetitive inhibitor ligands. Most importantly, lifetime measurements provide a means to distinguish signals from the free and bound species, and our measurements show that addition of PCP displaces ethidium from its binding site yielding a lifetime consonant with that of the free species. Hence, a ternary complex between ethidium, PCP and AChR is not formed, and the conclusions drawn from previous studies employing ethidium [32-35] should be re-evaluated in light of these findings.

Insight into the molecular nature of the ethidium binding site can be obtained from the examination of the fluorescence properties of bound ethidium. Studies of the mechanism of fluorescence enhancement for ethidium have suggested that the solvent environment is an important factor in dictating quantum yields [22]. Measurements of solvent and deuterium isotope effects on fluorescence lifetimes and quantum yields indicated that the primary mechanism for depopulation of ethidium's excited state is the quenching of the excited singlet state by solvent molecules [29]. From these observations, the long lifetime (22 ns) for ethidium bound at the noncompetitive inhibitor site can be explained by a substantial decrease in its accessibility to water molecules. The

similar long lifetime (22.2 ns) for ethidium intercalated between DNA bases has been attributed to a reduction in the rate of excited state proton transfer to solvent molecules [29]. Lifetimes of this magnitude are not observed when ethidium is dissolved in a wide range of hydrophobic solvents [2]. A large red shift in the excitation spectra for ethidium bound to the AChR is also observed for ethidium bound to DNA ($\lambda_{\text{max}} = 520 \text{ nm}$) and in several different solvents with dielectric constants less than water [22,29]. The 35 nm blue shift in the emission maxima of ethidium bound to the noncompetitive inhibitor site is also consistent with a restricted hydrophobic environment. In addition, the polarization data indicate that ethidium is strongly immobilized in the binding site. These observations suggest that, in the desensitized receptor state, the noncompetitive inhibitor binding site is primarily a hydrophobic pocket with limited accessibility to water. These conclusions are supported by study of a spin-labeled quaternary amine local anesthetic which showed that the spin label bound to the noncompetitive inhibitor site was strongly shielded from interactions with para-magnetic broadening agents in the aqueous phase [31].

The spectral characteristics of ethidium also reveal differences in the microenvironment of the noncompetitive inhibitor and agonist binding sites. Binding of ethidium to the agonist sites resulted in a 23 nm red shift in the excitation spectrum maximum compared to a 47 nm red shift for the noncompetitive inhibitor site. In addition, the fluorescent enhancement of ethidium bound to the agonist site is considerably less than the noncompetitive inhibitor site. These results indicate that the agonist/antagonist sites form a substantially less hydrophobic microenvironment than the noncompetitive inhibitor site. We have also used decidium as a fluorescent probe of both receptor sites. This compound also contains the phenylphenanthridium fluorophore, like ethidium, but in addition possesses a second quaternary amine linked via a ten-carbon alkyl chain. Decidium has been characterized as a nicotinic antagonist which binds preferentially to the agonist/antagonist sites, but also binds with lower affinity to the noncompetitive inhibitor site [47]. As in the case of ethidium, fluorescence excitation spectra of decidium also show a large red spectral shift when

bound to the noncompetitive inhibitor site, but show a smaller spectral shift when bound to the agonist site.

The identification of a unique ethidium binding site on the AChR that is allosterically regulated by agonists is consistent with ethidium binding to part of the ion channel structure. Our spectral data argue against the possibility that ethidium resides within the wide, aqueous portion of the channel present on the synaptic surface of the membrane [6]. Rather, the large spectral shifts, long lifetime and restricted motion of bound ethidium suggest that the phenylphenanthridium structure associates with hydrophobic portions of the presumed α -helical domains lining the transmembrane portion of the channel. Ethidium may thus act by creating a defect within the channel structure rather than by sterically occluding the channel. Although we cannot exclude the existence of a single allosteric site present on the periphery of the AChR complex that stabilizes an inactive receptor conformation, a single site located in contact with more than one subunit 40 is suggested by covalent labeling studies employing noncompetitive inhibitor ligands [15,30,17]. Our findings are inconsistent with ethidium altering receptor conformational equilibria due to nonspecific interactions with the AChR membranes, although other agents such as alcohols may act in this manner [4].

In this study we have sought to rigorously establish the stoichiometry and specificity of ethidium binding to the resting and desensitized states of the AChR. Additional studies probing the topology of the binding site and conformational changes associated with distinct receptor states are now possible. The structural mapping of the noncompetitive inhibitor site using fluorescence energy transfer should be feasible using ethidium and existing fluorescent probes of the agonist/antagonist binding sites.

TABLE I

Equilibrium Dissociation Constants for Noncompetitive Inhibitor Ligands Binding to the Torpedo AChR

Ligand	K_D^a (μ M)	$K_{R'A}^b$ (μ M)	K_{RA}^c (μ M)	$K_{RA}/K_{R'A}$ (μ M)	K_{des}^d (μ M)	n_H^a
Ethidium	0.25	0.36	~1,000	~2778	0.72	1.23
PCP	0.40	0.40	2.0	5.0	3.5	0.93
H8-HTX	0.044	0.031	-	-	-	0.98
Dibucaine	1.00	1.7	57.1	34.6	-	1.05

^aDetermined by fluorescence back titration of ethidium with competing ligands in the presence of 1 mM carbamylcholine and using $K_D = 0.25 \mu$ M for ethidium. ^bDetermined by competition binding with [³H]PCP in the presence of 1 mM carbamylcholine. ^cDetermined by competition binding with [³H]PCP in the presence of a 10-fold excess of α -toxin. ^dDetermined by the increase in [³H]ACh binding.

TABLE II

Fluorescence Spectral Properties of Ethidium Bound to the Noncompetitive Inhibitor and Agonist Binding Sites.

Ligands ^a	Excitation	Emission	K _D (μM)
	maxima ^c (nm)	maxima ^d (nm)	
Ethidium in buffer	480 ^a	635 ^a	---
AChR + CARB + ethidium	527 ^{a,c}	598 ^{a,c}	0.36
AChR + ethidium + PCP	504 ^{b,c}	614 ^{b,c}	11.0
AChR + CARB + ethid.+PCP	503 ^b	620 ^a	—
AChR + α-toxin+ethid.	503 ^b	620 ^a	—

^aConcentrations for the samples were: AChR, 1.0 μM α-toxin sites; ethidium, 1.0 μM; carbamylcholine, 0.5 mM; PCP, 1.0 mM; α-toxin, 10.0 μM. ^bConcentrations for the samples were: AChR, 1.0 μM α-toxin sites; ethidium 10.0 μM; PCP, 200 μM. ^cWavelength maxima obtained from difference spectra.

TABLE III

Fluorescence Lifetimes, Amplitudes, and Polarization for Ethidium Bound to AChR-Enriched Membranes^b

Ligands ^a	a_1	$\tau_1(\text{ns})$	a_2	$\tau_2(\text{ns})$	a_1/a_2	χ^2/N	P^c
Ethidium in buffer	-	1.7	-	-	-	6.5	.02
AChR + CARB + ethidium	-	22.2	-	-	-	2.0	.41
AChR+CARB+ethid.+PCP	.88	1.4	.12	21.5	7.5	8.6	.22
AChR + α -toxin + ethid.	.88	1.5	.12	22.1	7.3	5.5	.27
AChR + ethidium	.75	2.0	.25	20.6	3.0	1.8	-

^aConcentrations for the above samples were: AChR, 1.0 μM α -toxin sites; ethidium, 1.0 μM ; carbamylcholine, 0.5 mM; PCP, 1.0 mM; α -toxin, 5.0 μM . ^bExcitation and emission bands were selected with a Corning 7-54 and 3-70 filter, respectively. ^cPolarization (P) was determined as described in the Methods section.

Figure 1: Inhibition of the binding of [3 H]PCP by ethidium and its allosteric regulation by agonist occupation.

Acetylcholine receptor-enriched membranes ($1.0 \mu\text{M}$ α -toxin sites) and $1.0 \mu\text{M}$ [3 H]PCP were incubated with either 1.0 mM carbamylcholine (\blacksquare) or $10 \mu\text{M}$ α -toxin (\blacktriangle) and ethidium at the specified concentrations. Specifically bound [3 H]PCP was determined by subtracting the binding in the presence of 1.0 mM nonradioactive PCP from the total binding. The two competition curves have been normalized to 100% binding to facilitate comparison of ethidium affinities in the resting and desensitized receptor states. The solid lines through the data were fit by nonlinear least squares analysis assuming a single class of binding sites.

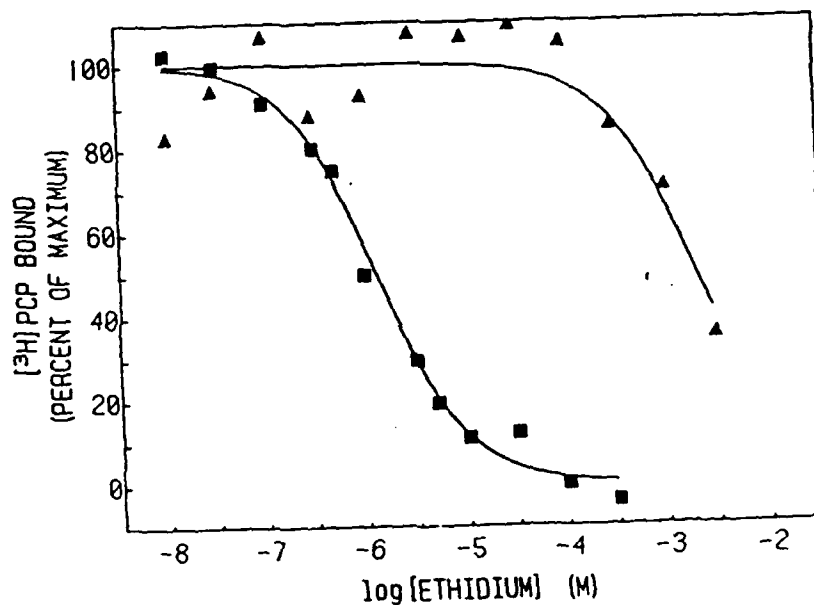


Figure 2. The influence of ethidium and PCP on the binding of [3 H]acetylcholine to AChR-enriched membranes.

(A) Effects determined by fractional occupation of agonist binding sites in the absence of added noncompetitive ligand. AChR-membranes were pretreated with 0.1 mM DFP for 1 hr. The membranes (25 nM α -toxin sites) were incubated with 25 nM [3 H]ACh at the specified concentrations of PCP (■) and ethidium (○). Free and bound [3 H]ACh were separated by filtration as described under Materials and Methods.

(B) Inhibition of [3 H]ACh binding by ethidium. DFP-pretreated AChR-enriched membranes (100 nM α -toxin sites) were incubated with 100 nM [3 H]ACh either in the absence (●) or presence of 250 μ M PCP (■) at the specified concentrations.

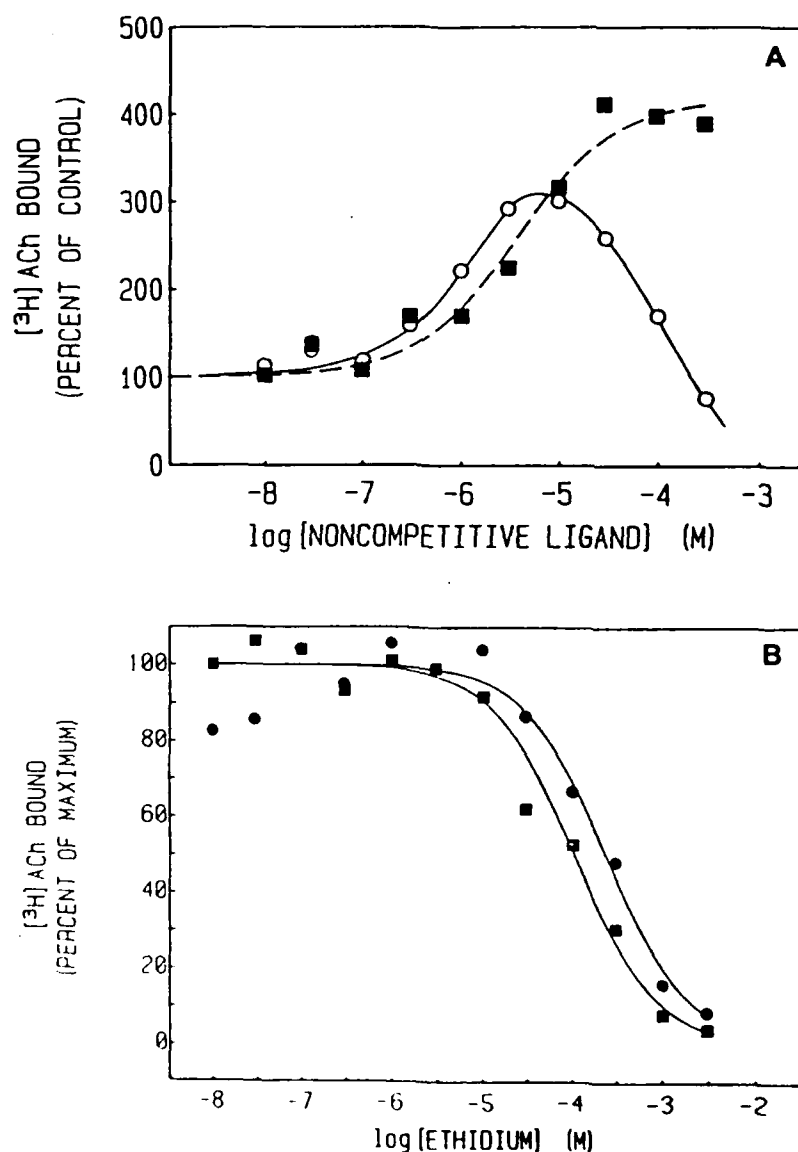


Figure 3. Effect of agonists, antagonists and noncompetitive inhibitors on the fluorescence spectra of ethidium bound to AChR-enriched membranes.

(A) Corrected fluorescence excitation spectra of: 1) AChR-membranes ($1.0 \mu\text{M}$ α -toxin sites) in the presence of 1 mM carbamylcholine and $1.0 \mu\text{M}$ ethidium, 2) AChR membranes ($1.0 \mu\text{M}$ α -toxin sites), preincubated with $10.0 \mu\text{M}$ α -toxin, and $1.0 \mu\text{M}$ ethidium, 3) AChR membranes ($1.0 \mu\text{M}$ α -toxin sites), 1 mM carbamylcholine; $1.0 \mu\text{M}$ ethidium, and $200 \mu\text{M}$ PCP. All solutions were in 100 mM NaCl, 10 mM NaPO_4 , pH 7.4. Emission was measured at 593 nm, 4) $1.0 \mu\text{M}$ ethidium in buffer, 5) $10 \mu\text{M}$ ethidium, AChR-membrane ($5.0 \mu\text{M}$ in α -toxin sites) and PCP ($200 \mu\text{M}$).

(B) Corrected fluorescence emission spectra of samples 1, 2, 3, 4 and 5 as described above in (A). Excitation wavelength was 480 nm.

(C) Corrected fluorescence emission spectra of samples 1, 2, 3, 4 and 5 as described above in (A). Fluorescence was excited at 290 nm, allowing energy transfer from AChR tryptophan residues to ethidium.

(D) Fluorescence emission difference spectra of ethidium bound to the noncompetitive inhibitor site. Difference spectra obtained using excess PCP to define nonspecific binding and (1) exciting at 480 nm or (2) exciting at 290 nm. Difference spectra obtained using α -toxin to define nonspecific binding, and (3) exciting at 480 nm, or (4) exciting at 290 nm. Difference spectra of ethidium bound to the agonist site were obtained by subtracting the spectrum of (5) in the presence of $10.0 \mu\text{M}$ α -toxin. All spectra have been normalized with respect to their maximum intensity for comparison of emission maxima and spectral shape.

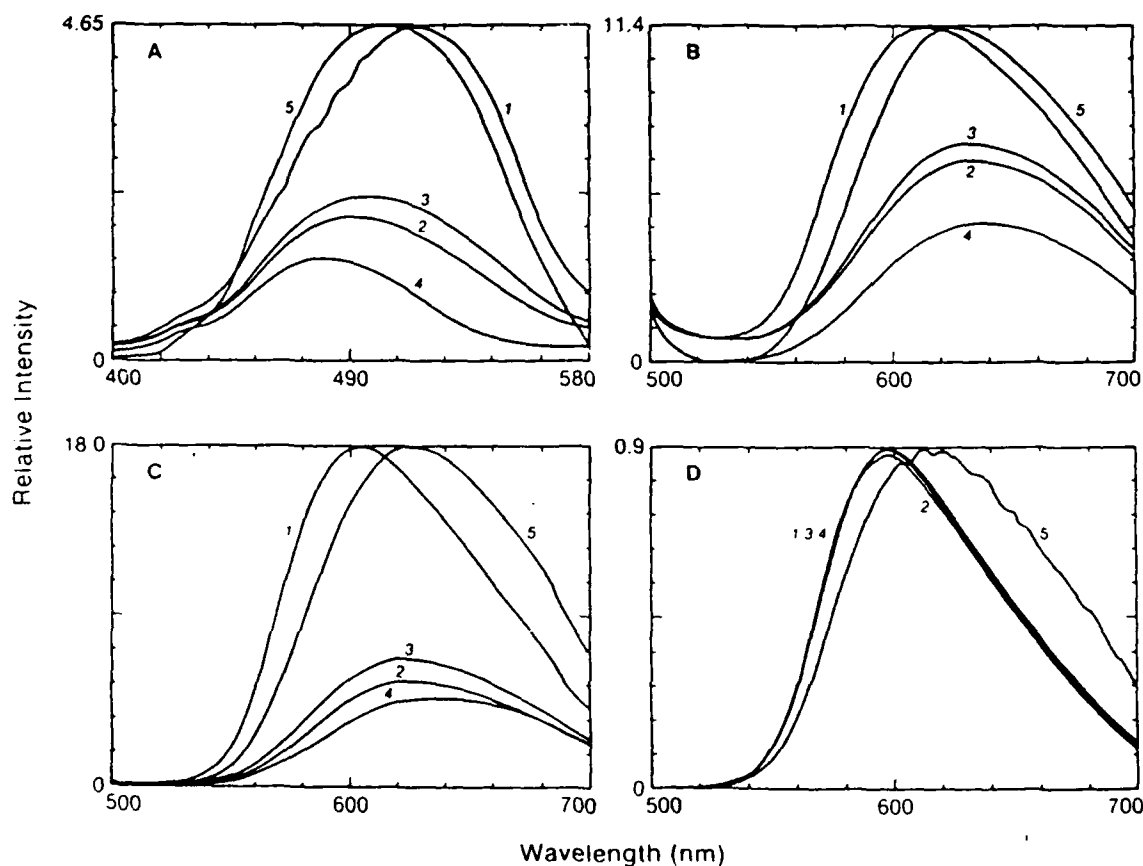


Figure 4.

(A) Fluorescence titration of AChR-enriched membranes with ethidium in the presence of carbamylcholine. AChR-membranes ($0.2 \mu\text{M}$ α -toxin sites) were equilibrated with 0.5 mM carbamylcholine. Titrations were carried out in 100 mM NaCl , 10 mM NaPO_4 , pH 7.4 at 25°C . (O-O), AChR and carbamylcholine; (Δ - Δ) AChR, carbamylcholine, and 1 mM PCP , (\blacktriangle - \blacktriangle) AChR, carbamylcholine and $10.0 \mu\text{M}$ α -toxin.

(B) Scatchard plot of the fluorescence titration of AChR with ethidium in the presence of carbamylcholine. The specific binding of ethidium was calculated from the data in (A) was found to be identical using either the nonspecific binding determined in the presence of 1 mM or $10 \mu\text{M}$ PCP or $10 \mu\text{M}$ α -toxin. Calculations are based upon saturation of binding sites resulting in 1 mole of ethidium bound per 2 moles α -toxin binding sites.

(C) Stoichiometry determined from the fluorescence titration of AChR-enriched membranes in the presence of carbamylcholine with ethidium. AChR-enriched membranes ($2.0 \mu\text{M}$ α -toxin sites) were equilibrated with 0.5 mM carbamylcholine. Other experimental conditions as described in (A). (O-O) total fluorescence, (Δ - Δ) nonspecific binding determined in the presence of 1 mM PCP , (\bullet - \bullet) specific fluorescence changes. The solid lines extrapolated from the stoichiometric region of binding and the level achieved at saturation intersect at $1.0 \mu\text{M}$ ethidium, indicating 1 mole of ethidium binding sites per 2 moles α -toxin binding sites.

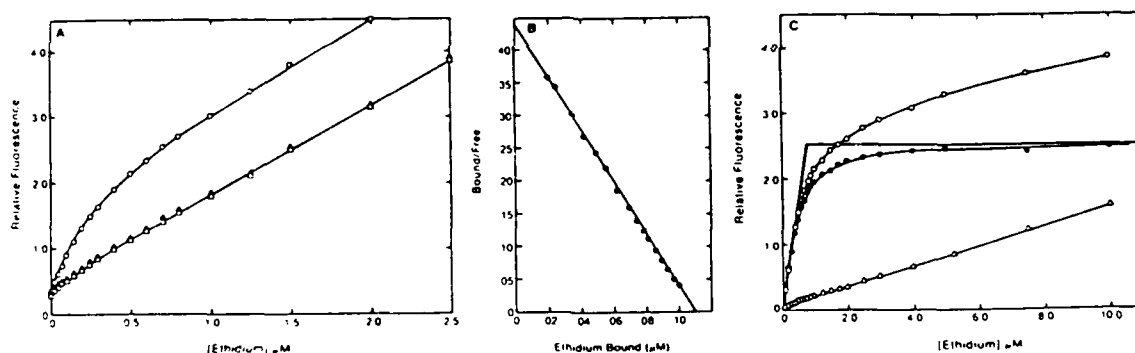


Figure 5.

(A) Dissociation of the ethidium-AChR complex in the presence of carbamylcholine by PCP. Incremental additions of PCP were made to a solution containing AChR-membranes ($1.0 \mu\text{M}$ α -toxin sites), $1.0 \mu\text{M}$ ethidium, and 0.5 mM carbamylcholine. Titration profile derived from measurement of ethidium fluorescence ($\lambda_{\text{ex}} = 500 \text{ nm}$, $\lambda_{\text{em}} = 593 \text{ nm}$).

(B) Hill plots of the competitive dissociation of ethidium from AChR-membranes in the presence of carbamylcholine by noncompetitive inhibitor site ligands. Experimental conditions are as in (A), above. Data are plotted logarithmically where $[C]$ and $[E]$ are concentrations of the competing ligand and ethidium, respectively. f_E denotes the initial fluorescence in the absence of competing ligands, f_c denotes the fluorescence when ethidium is completely displaced from the AChR, and f denotes the fluorescence observed at any given concentration of competing ligand during the titration (O-O) PCP, (■-■) H8-HTX, (●-●) dibucaine.

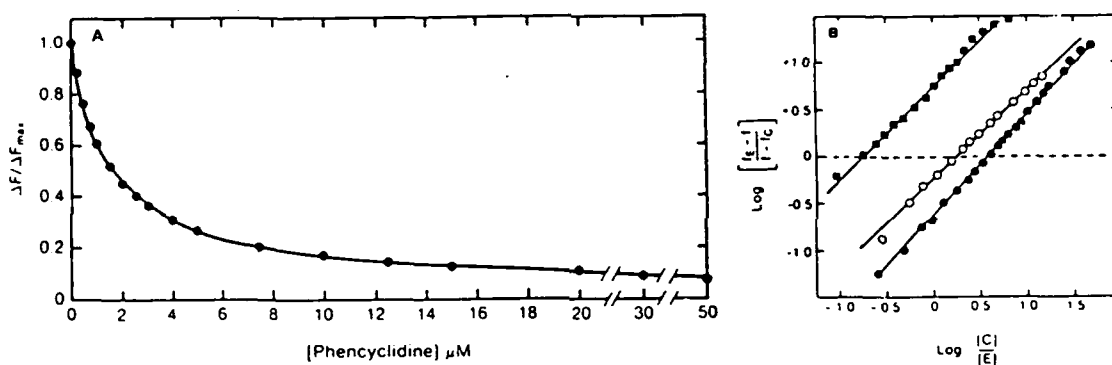


Figure 6. The effect of association of carbamylcholine on the binding of ethidium to AChR-enriched membranes.

Torpedo AChR membranes ($1.0 \mu\text{M}$ α -toxin sites) were equilibrated with $1.0 \mu\text{M}$ ethidium prior to incremental addition of carbamylcholine. The titration profile was obtained by measurement of ethidium fluorescence ($\lambda_{\text{ex}} = 290 \text{ nm}$, $\lambda_{\text{em}} = 594 \text{ nm}$). Nonspecific changes in fluorescence were measured in an equivalent sample containing either 0.5 mM PCP or $10.0 \mu\text{M}$ μ -Toxin. The solid line through the data is a theoretical curve calculated from the law of mass action and assuming $1.0 \mu\text{M}$ carbamylcholine binding sites.

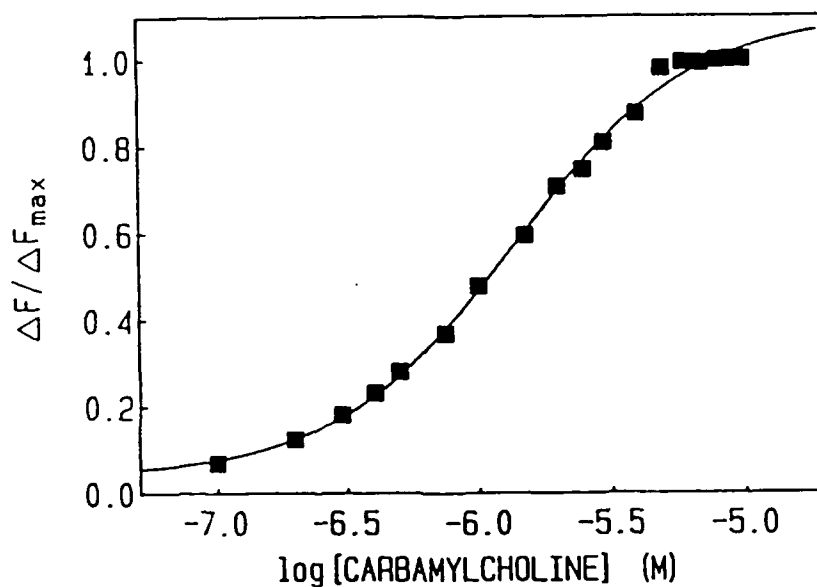
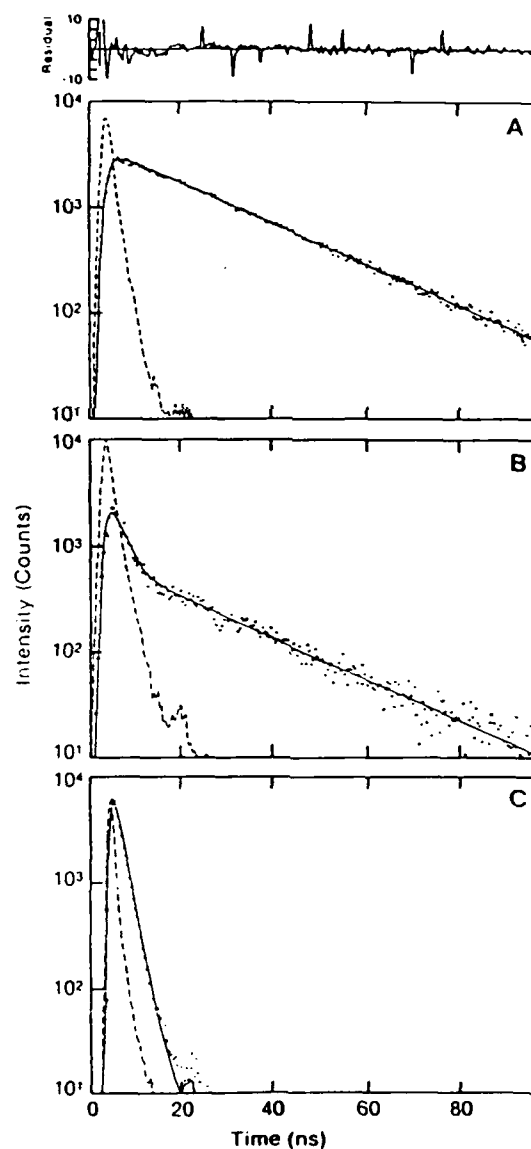


Figure 7. Fluorescence lifetime measurements of ethidium bound to AChR-enriched membranes.

The fluorescence lifetime of ethidium was measured using excitation in the UV absorption band in the following solutions: A) 1.0 μ M α -toxin sites AChR enriched membranes, 0.5 mM carbamylcholine and 1.0 μ M ethidium; (B) 1.0 μ M α -toxin sites AChR enriched membranes, 0.5 mM carbamylcholine and 1.0 mM PCP; (C) 10.0 μ M ethidium in 100 mM NaCl, 10 mM NaPO₄, pH 7.4.

Each panel shows the lamp pulse (dashed line), the raw data (dotted line) and the computer-calculated decay curve (solid line) obtained from deconvolution of the experimental decay with the lamp pulse by the method of moments. The residual analysis (χ^2/N) for deviation of the calculated curve from the data is shown for sample A.



SECTION II

MODULATION OF RECEPTOR STATE WITH BUTANOL

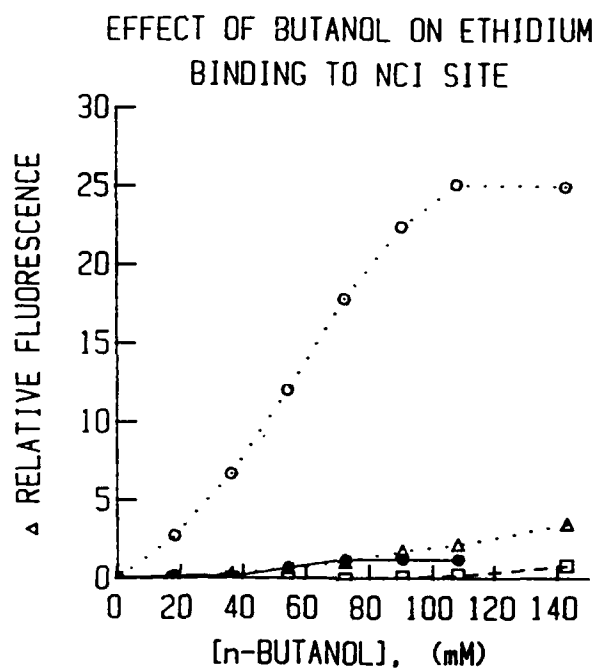
Since the absorption spectra of ethidium overlaps with FITC, we wanted to use energy transfer techniques to measure the distance between the NCI site and the agonist/antagonist sites using ethidium as an acceptor, bound to the NCI site and FITC-toxin, as a donor, bound to the agonist/antagonist sites. However, we have only observed ethidium binding to the NCI site when an agonist like carbachol was bound to the agonist/antagonist sites. In other words, the receptor had to be in the desensitized state before ethidium would bind. Consequently, we attempted to convert the α -toxin-bound AChR to the desensitized state with butanol. Butanol was chosen because it, like other aliphatic alcohols, converts the AChR to the desensitized state by interacting at sites other than the NCI and agonist/antagonist sites [45,46]. Since butanol interacts at sites other than the NCI and agonist/antagonist sites, we thought butanol might stabilize the α -toxin-bound AChR in the desensitized state. To test this idea, we titrated butanol into fluorometer cuvettes containing ethidium in buffer and appropriate combinations of AChR, native α -toxin, and PCP. Since the quantum yield of ethidium increases about fourteen fold when it binds to the AChR, we monitored ethidium fluorescence as an index of its association with the AChR. The results of these experiments are shown in Fig. 8. As would be predicted if butanol converts the receptor to the desensitized state, ethidium fluorescence increased in the presence of the AChR with increasing concentrations of butanol. Also, as would be predicted if the increase in fluorescence was dependent on ethidium binding to the NCI site, excess PCP (100 μ M) blocked this effect. Unfortunately, preincubation of the AChR with native α -toxin also blocked the butanol-induced ethidium binding, strongly suggesting that α -toxin stabilizes the AChR into the resting state. Other samples without AChR show that butanol has little direct effect on ethidium fluorescence.

To test whether butanol could "lock" the AChR into the de-sensitized state, butanol (0.072

M) was added to ethidium ($0.4 \mu\text{M}$) and AChR ($0.2 \mu\text{M}$ in α -toxin sites) before and after addition of α -toxin (data not shown). We found that no matter when the butanol was added, α -toxin converted the AChR into a state in which ethidium displays little affinity toward the receptor.

The above results are, at face value, inconsistent with what is generally thought about the interaction of α -toxin with the AChR. It has been generally thought that α -toxin binds with equal affinity to the resting and desensitized states. This is based on the observation that the bimolecular association rate of α -toxin binding to the AChR in the resting and desensitized state are about the same, so it was assumed that the dissociation constants of α -toxin towards the two states of the AChR were also the same. This may not be the case. α -Toxin may dissociate more rapidly from the AChR in the desensitized state than the resting state. To explain all the results will require the measurement of the effect of butanol on the dissociation of α -toxin for the AChR. (In some preliminary studies we have observed butanol to increase the dissociation rate of α -toxin from the AChR.)

Figure 8. Effect of butanol on binding of ethidium to the AChR-enriched membranes; ○-○ Ethidium (0.4 μ M) and AChR (0.4 in α -toxin sites; ●-●, Ethidium, AChR and α -toxin (1 μ M); Δ - Δ Ethidium only; □-□ Ethidium, AChR and PCP (1 mM).



SECTION III

A. PROGRESS REPORT ON EFFORTS TO SITE SPECIFICALLY LABEL COBRA α -TOXIN WITH FITC

One of our major goals is to develop a "library" of site-specifically labelled α -toxins with which to examine the spatial relationships between drug binding sites and the surface of the AChR by utilization of fluorescence energy transfer and quenching techniques. In our first annual report, we reviewed our efforts in the first year of the project to label α -toxin with FITC, EITC and TRITC. What we learned in the first year was that we could redirect some of the labelling to sites other than lysine 23 using reversible modification of the primary amino groups before labelling with the fluorescent isothiocyanate derivatives. However, we only achieved limited success in separating the various monofluorescent conjugates. The techniques we used to resolve the monoconjugates included CM-52 and BioRex 70 ion exchange chromatography and column isoelectric focusing. Because of the inadequate resolution of these techniques, we decided to utilize preparative immobilized-pH-gradient isoelectric focusing gels [12]. What is unique about these gels is that the ampholytes are covalently bonded to the acrylamide. No diffusion of the ampholytes occurs so that very narrow pH gradients can be formed and peptides can focus in sharper bands. The problem with this technique is that it is relatively new and not all the parameters have been worked out.

After overcoming many problems, we have been able to resolve what appear to be all six FITC-toxin monoconjugates on immobilized-pH-gradient isoelectric focusing gels [12]. A photograph of the fluorescence of FITC-toxin monoconjugates on a 0.5 cm thick is shown in Fig. 9. We have labelled these bands 1, 2, 3, 3a, 4 and 5. The major band is 5 and FITC-lysine-23 α -toxin comigrates with this band strongly suggesting that band 5 is labelled at lysine 23. Bands 1 and 2 are the next most abundant bands, and we have isolated about 100 μ g of each of these bands. Microsequencing of the first twenty amino acids in these two bands indicate that they are not labeled at the N-terminus or lys-12. Resolution of a thermolysin digest of band 2 on a C18 HPLC

column yielded one major peak of fluorescein fluorescence (see Fig. 10). The sequence of this peptide was arg-FITC-lys-arg-pro, which indicates that Band 2 is labelled at lys 69. We are about a month away from determining the site of labelling of Band 1.

B. CHARACTERIZATION OF FITC-TOXIN BANDS 1, 2, AND 5.

Binding of Bands 1, 2 and 5 to the membrane associated AChR is associated with -7%, -20% and +140% change in fluorescein fluorescence, respectively. The bimolecular association rate constants for binding to the AChR are 2.7, 4.3 and $1.3 \text{ M}^{-1} \text{ s}^{-1}$, respectively. Iodine quenching of steady fluorescence and fluorescence lifetime analysis indicate that the fluorophores associated with each of these three FITC-toxin conjugates are solute accessible either when the monoconjugates are free in solution or bound the AChR. Since Band 5 FITC-toxin is labelled at lysine 23 and Band 2 at lysine 69, we can develop some constraints on a possible model of how cobra α -toxin rests on the surface of the AChR.

Figure 9. Photograph of the fluorescence of FITC-toxin monoconjugates resolved on a 0.5 cm thick LKB Immoboline gel.

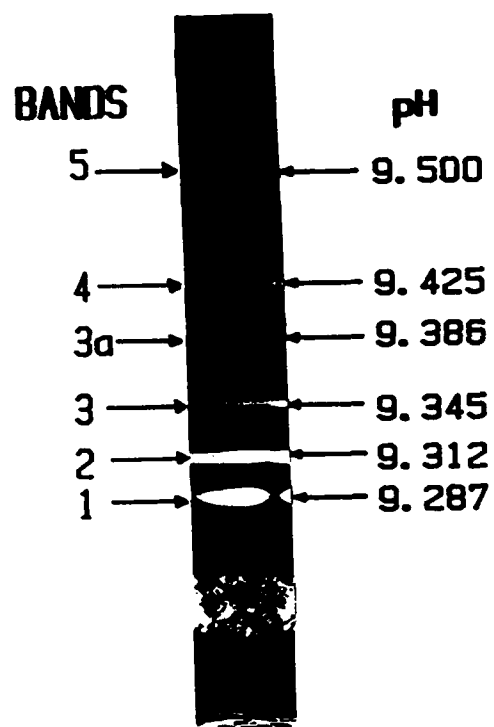
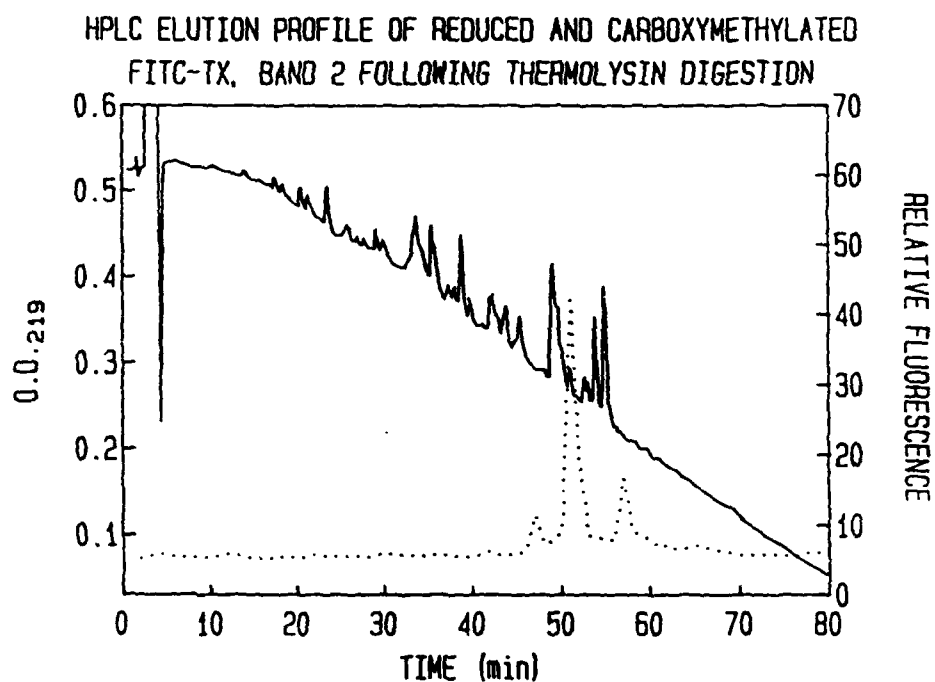


Figure 10. High pressure liquid chromatography elution profile of reduced and S-carboxymethylated peptides from FITC-toxin Band 2 following thermolysin digestion. Solid line, 219 extinction; dashed line, relative fluorescence. Elution was accomplished with a gradient of 0-40% acetonitrile in 0.1% trifluoroacetic acid.



REFERENCES

1. Aronstam, R.S., Eldefrawi, A.T., Pessah, I.N., Daly, J.W., Albuquerque, E.X. and Eldefrawi, M.E. (1981) *J. Biol. Chem.* 256:2843-2950.
2. Atherton, S.J. and Beaumont, P.C. (1984) *Photobiochem. Photobiophys.* 8:103-113.
3. Blanchard, S.G., Elliott, J. and Raftery, M.A. (1979) *Biochemistry* 18:5880-5885.
4. Boyd, N.D. and Cohen, J.B. (1984) *Biochemistry* 23:4023-4033.
5. Boyd, N.D. and Cohen, J.B. (1980) *Biochemistry* 19:5344-5353.
6. Brisson, A. and Unwin, P.N.T. (1985) *Nature* 315:474-477.
7. Brown, R.D. and Taylor, P. (1982) *Mol. Pharmacol.* 23:8-16.
8. Burgermeister, W., Catterall, W. and Witkop, B. (1977) *Proc. Natl. Acad. Sci. USA* 74:5754-5758.
9. Claudio, T., M. Ballivet, J. Patrick and S. Heinemann. 1983. *Nature (Lond.)*, 80:1111-1115.
10. Cohen, J.B., Medynski, D.C. and Strand, N.P. (1985) in *Effects of Anesthesia*, Covino, B.J., Fozzard, H.A., Rehder, K. and Strichartz, G., eds. pp. 53-63, American Physiological Society, Bethesda, MD.
11. Elliot, J. and Raftery, M. (1979) *Biochemistry* 18:1868-1877.
12. Gianazza, E., Chillemi, F., Duranti, M. and Righetti, P.G. (1983) *J. Biochem. Biophys. Methods* 8:339-351.
13. Grunhagen, H.-H. and Changeux, J.-P. (1976) *J. Mol. Biol.* 106:497-516.
14. Heidmann, T. and Changeux, J.-P. (1979) *Eur. J. Biochem.* 94:281-296.
15. Heidmann, T., Oswald, R.E. and Changeux, J.-P. (1983) *Biochemistry* 22:3112-3127.
16. Johnson, D., Voet, J.G. and Taylor, P. (1984) *J. Biol. Chem.* 259:5717-5725.
17. Kaldany, R.R. and Karlin, A. (1983) *J. Biol. Chem.* 258:6232-6242.
18. Karlsson, E., Arnberg, H. and Eaker, D. (1971) *Eur. J. Biochem.* 21:1-16.
19. Kistter, J., Stroud, R.M., Klymkowsky, M.W., Lalancette, R.A. and Fairclough, R.H. (1982)

37:371-383.

20. Koblin, D.R. and Lester, H. (1979) *Mol. Pharmacol.* 15:559-580.
21. Krodel, E.K., Beckman, R.A. and Cohen, J.B. (1979) *Mol. Pharmacol.* 15:294-312.
22. LePecq, J.B. and Paoletti, C. (1967) *J. Mol. Biol.* 27:87-106.
23. Magazanik, L.G. and Vyskocil, F. (1976) in *Motor Innervation of Muscle* (S. Thesleff, ed.) Academic Press, pp. 151-176.
24. Munson, P.J. (1983) *Methods Enzymol.* 92:543-576.
25. Neher, E. and Steinbach, J.H. (1979) *Mol. Pharmacol.* 15:559-580.
26. Neubig, R.R., Krodel, E.K., Boyd, N.D. and Cohen, J.B. (1979) *Proc. Natl. Acad. Sci. USA* 76:690-694.
27. Noda, M., Takahashi, H., Taube, T., Toyosata, M., Furutani, Y., Hirsoe, T., Asai, M., Inayama, S., Miyata, T. and Numa, S. (1982) *Nature (Lond.)* 299:793-797.
28. Noda, M., Takahashi, H., Taube, T., Toyosato, M., Kikyotani, S., Hirose, T., Asai, M., Takashima, H., Inayama, S., Miyata, T. and Numa, S. (1983) *Nature (Lond.)* 301:251-255.
29. Olmsted, J. III and Kearns, D.R. (1977) *Biochemistry* 16:3647-3654.
30. Oswald, R.E. and Changeux, J.-P. (1981) *Biochemistry* 20:7166-7174.
31. Palma, A., Herz, J.M., Wang, H.H. and Taylor, P. (1986) submitted for publication.
32. Quast, U., Schimerlik, M., Lee, T., Witzemann, V., Blanchard, S. and Raftery, M.A. (1978) *Biochemistry* 17:2405-2415.
33. Quast, U., Schimerlik, M. and Raftery, M.A. (1979) *Biochemistry* 18:1891-1901.
34. Schimerlik, M., Quast, U. and Raftery, M.A. (1979a) *Biochemistry* 18:1884-1890.
35. Schimerlik, M.I., Quast, U. and Raftery, M.A. (1979b) *Biochemistry* 18:1902-1906.
36. Schmidt, J. and Raftery, M.A. (1973) *Anal. Biochem.* 52:349-355.
37. Sine, S. and Taylor, P. (1982) *J. Biol. Chem.* 257:8106-8114.
38. Sobel, A., Heidmann, T., Cartaud, J. and Changeux, J.-P. (1980) *Eur. J. Biochem.* 110:13-33.

39. Taylor, P. and Lappi, S. (1975) *Biochemistry* 14:1989-1997.
40. Taylor, P., Weiland, G., Sine, S., Chignell, C.F. and Brown, R.D. (1980) in *Molecular Mechanisms of Anesthesia* (B.R. Fink, ed.) pp. 175-187, Raven Press, New York.
41. Terrar, D.A. (1974) *Br. J. Pharmacol.* 51:259-268.
42. Weiland, G., Georgia, B., Wee, V.T. Chignell, C.F. and Taylor, P. (1976) *Mol. Pharmacol.* 12:1091-1105.
43. Weiland, G.A., Georgia, B., Lappi, S., Chignell, C.F. and Taylor, P. (1977) *J. Biol. Chem.* 252:7648-7656.
44. Yguerabide, J. and Yguerabide, E.E. (1984) In *Optical Techniques in Biological Research* (J. Doyle, ed.), Academic Press, pp. 181-290.
45. Young, A.P. and Sigman, D.S. (1981a) *Mol. Pharmacol.* 20:498-505.
46. Young, A.P. and Sigman, D.S. (1981b) *Mol. Pharmacol.* 20:505-510.
47. Johnson, D.A., Brown, R.D., Herz, J.M., Berman, H.A., Andreason, G.L. and Taylor, P. (In preparation.)